

Single-Band Infrared Texture-Based Image Colorization

Tomer Hamam, Yedidyah Dordek, Deborah Cohen

Signal and Image Processing Laboratory (SIPL)

Department of Electrical Engineering, Technion – Israel Institute of Technology

Technion City, Haifa, 32000, Israel

Abstract—Infrared (IR) imaging has a wide variety of applications such as night vision detection and tracking, meteorology radiometers and spectroscopy techniques. An infrared image is a monochrome image, usually presented in grayscale. It has been proved that colorization of IR images can reduce human error and speed up reaction time. Most previously suggested coloring methods use a reference color image, whose characteristic features differ drastically from IR ones. These differences make those features less pertinent to the coloring process. In this paper, we present a novel texture-based method for automatically coloring IR images. The method uses a reference (source) color image, which is selected from a database, built in advance containing various natural scenes. The source image is selected using a texture-matching algorithm that searches for a resemblance to the IR (target) image. The source and target images are divided into texture-based segments and a color segment best match is found for every IR segment. The coloring process is performed for each pair of IR-color segments, and exploits global as well as local features. Results show that our method produces more natural-looking images than achieved heretofore.

Index Terms—infrared, colorization, texture.

I. INTRODUCTION

Infrared (IR) imaging processes thermal emissions from various surroundings, producing a powerful vision system that overcomes some of the natural limits of human sight. Exploitation of such data is extremely useful for functioning at night time or in other poorly lighted conditions. Today, IR systems are more common than ever before because of decreasing prices. They are found in military as well as civilian tracking and surveillance devices. Among the IR imaging systems, there are two types of devices: Those that have single-band sensors sensitive to a limited range of emitted radiation wavelengths and those that exploit a larger portion of the electromagnetic spectrum, combining more than one band. In this work, we focus on single-band systems, which are more commonly used due to their lower prices.

As the IR acquired image is based on temperature differences only, it is monochromatic and usually presented in grayscale. That aspect is a serious drawback, since the purpose of these systems is to facilitate clear and quick recognition of their surroundings, which cannot always be achieved using a grayscale image. Indeed, experimental data indicate that object

recognition is dependent on stored knowledge of the object's chromatic characteristics [1]. It was shown [2] that the optimal reaction time and maximum accuracy in natural scene imagery are achieved for daytime natural colors, better than their grayscale version. In [3] it was suggested that the use of false colored night vision images (created by adding colors, which are not necessarily the original ones, to the grayscale image) significantly improves scene comprehension and reaction times in tasks that involve scene segmentation and classification. However, color mapping that produces counterintuitive (unnatural-looking) results may lead to inferior performance compared even with grayscale images. Thus, it is critical to give night vision imagery an intuitively meaningful and consistently-colored appearance [4].

IR images differ substantially from color images. A color camera gathers visible light reflected off objects and captures it as a color image. On the other hand, IR imaging processes thermal radiation, producing a grayscale image of captured item's temperature. This inherent distinction between the nature of color and IR images is a major challenge when one goes to colorize an IR image. Another main factor in this process that needs to be considered is the lack of an established objective error measure, since a single grayscale value can be matched, with no clear mapping criterion, to several different colors.

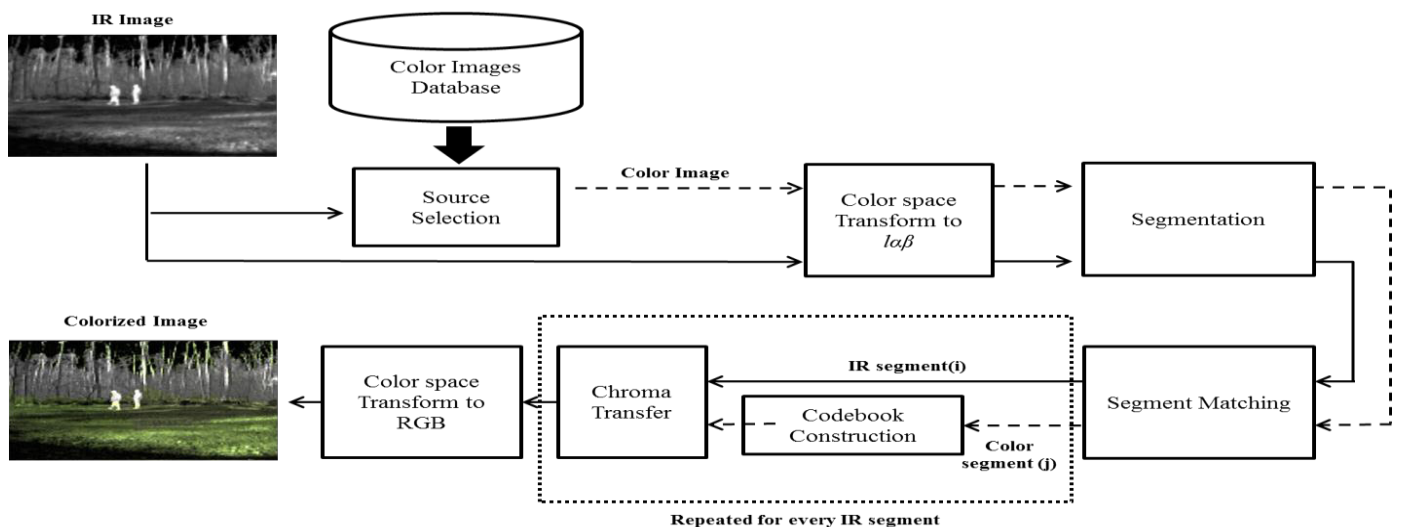
A prominent method for the colorization of single-band IR images was introduced by Toet [5]. In this method, a reference (source) color image is used to globally match between IR and color pixels. First, a group of color pixels is randomly selected to form a codebook. Next, the first and second-order statistics (mean and standard deviation) of the codebook's pixels are found and matched to those of every IR pixel followed by transforming corresponding chromaticity in a decorrelated color space. The reference image does not need to be of the exact scene; however, it should resemble the IR image and contain similar properties. Toet's method has several drawbacks. Firstly, the source color image is selected manually, which is relatively cumbersome and may be impractical for usage in situations with varying scenery. Secondly, an inconsistency in object's colors can be produced due to the usage of global information when matching IR and color pixels (i.e., Color from different parts of the source image can be found out of context in the rendered outcome).

Thirdly, the pixel-matching process relies on features that are not necessarily correlated between the color image and the IR image. On the contrary, textural features are similarly expressed in both images, and similar texture tends to have similar colors.

chromatic information is transferred and the image is transformed back to RGB. This process is depicted in Figure 1.

II. INFRARED COLORIZATION

In light of the inherent differences existing between IR and color images, texture features appear to be a promising tool in the matching process of both images. The proposed technique exploits those properties at three distinct levels: The image level, the image segments level and the pixel level. First, the source image is automatically selected based on the textures in the scenery. Then, the IR image is colored segment-wise, with each segment composed mainly of one prominent texture, and finally every pixel inherits chromatic values from the source image based on local features that are mostly texture-based. Let us review the considerations lying behind each of those steps of the algorithm. In the first level, we manipulate the textural information to select a source image similar to the IR one in terms of scenery. Since we do not have color data in the IR image, we consider the information obtained from IR radiance as if it is regular image brightness. We then collect image statistics in different regions corresponding to different textures. This textural information allows us to select from a large database a source image whose brightness information resembles the IR target image. In the first stage, we use a more accurate, but computationally intensive descriptor, since most computations at this stage are performed off-line.



adapted to online computation. After the segment matching process is complete, we now use texture features at the pixel level in each segment of the IR image. In this stage, each IR pixel is matched to a color one from the corresponding color segment. For that task, we need a descriptor of a more local nature that has low computation costs to allow online work at the pixel level. In the following sections, we present in more detail the three texture descriptors that are suited for the texture matching tasks mentioned above.

B. Source Selection

The source selection process aims to match the target IR image with a corresponding reference color image that resembles the target in terms of scenery. The selection process is based on a global texture descriptor that uses multifractal analysis in a multi-orientation wavelet pyramid [11]. The descriptor combines information from both spatial and frequency domains and has shown in previous work strong ability for representing natural textures because of their fractal structures [12][13][14]. In order to capture the features in textures in different spatial locations, the image is divided into sub-images. A division to 16 sub-images was chosen so that each sub-image contains roughly one main texture element. Every sub-image I , is used to generate a descriptor as follows: A discrete wavelet transform (DWT) is computed by, decomposing I into one low-level frequency channel $D_j(I)$ with the coarsest scale and multiple high frequency channels of multiple scales $W_{k,j}(I)$, $k = 1, 2, 3$, $j = 1, 2 \dots J$ where J is the number of scales (We use $J=3$ as in [7]). In order to classify textures efficiently, a multifractal spectrum analysis (MFSA) is used as a statistical measure of the wavelet coefficients. MFSA was originally used in the study of fractal objects [15], where it serves to analyze complex or irregular geometric objects. The main aim behind fractal analysis is to analyze the object in terms of irregularity. In our case, we use plain fractal dimension, which is a statistical measurement of how a given point set (E) appears to fill the space as one zooms towards finer scales. A common approximation for this measure is called the box-counting fractal dimension, which is defined as follows: Given a 2D space covered by a mesh of $n \times n$, and a set of points $E \in R^2$ that is on the mesh, we define the number $\#(E, \frac{i}{n})$ as the number of $\frac{i}{n}$ mesh squares that intersect with E for $i = 1, 2, 3, \dots, n$. The definition of fractal dimension when using the box-counting method is then given by:

$$\dim(E) = \lim_{i \rightarrow n} \frac{\log \#(E, \frac{i}{n})}{-\log(\frac{i}{n})}. \quad (1)$$

One prominent advantage of the MFSA is that it classifies well objects of fractal nature, which is the case in many natural textures. Secondly, it is scale invariant, since it measures differences in intersections between several scales.

In order to save real time computations, the database is

processed off-line, and the descriptor for every image in the database is a vector of its sub-images fractal features. The IR image is processed in a similar way to generate a descriptor vector. The source selection is then performed by finding the color vector that yields a minimum square error.

C. Color Space Transformation

In order to avoid artificial colorization effects when we transfer the chromatic values, the process has to be performed in a space in which the chromatic and luminance channels are all uncorrelated. Following the work of Ruderman's [16], we use the $l\alpha\beta$ decorrelated color space, where l stands for the luminance channel and α, β for the chromatic channels. The transformation between RGB and $l\alpha\beta$ is the same as in Reinhard's work [17], where he used Ruderman discoveries to perform simple tasks of colorization. In the case of the IR image, we compute only the luminance l using the IR intensity for all three RGB channels.

D. Image Segmentation

In order to allow the colorization process to exploit regional information, we segment both images and match each IR segment to a color one. The colorization will then be performed on each pair of matched segments separately. We propose to segment the images according to texture properties. A texture segment is composed of pixels of similar texture and adjacent coordinates (x, y) , in the image. The segmentation of the color image is constructed by clustering the image pixels according to their $l\alpha\beta$ and (x, y) coordinates. Dividing into 16 segments is usually enough to obtain one prominent texture in each segment. Since the IR is monochromatic, a simplified version of the same method is used. This time, the only parameters used for the segmentation are the luminance value and the (x, y) coordinates.

Prior to the color transformation, we need to allocate a corresponding segment to each IR segment in the color image. For example, although both sky and grass could have a small area with similar smoothness, i.e., the same local properties, the grass is less probable to inheriting the sky's blue colors when segment matching is done beforehand. To perform the allocation, textural representation of each segment is extracted by using the histogram of gradients (HOG) method [18]. For each pixel in the segment, gradients of its neighborhood are computed, and a histogram vector of those gradients' directions represents the segment. The HOG method corresponds to the second level of texture descriptors, which we introduced in section II.A. It captures the directivity and periodicity of the texture in a way that is able to characterize textures when the number of textures is limited, as in our case. The HOG process is repeated for all segments in both IR and color images, yielding representing vectors for all the segments. To complete this stage we match every vector of an IR segment to a vector of a color segment according to minimal Euclidean distance.

E. Constructing Chromatic Codebook

Once the segment matching between the color and the IR images is done, we construct a chromatic codebook. The codebook is constructed for every segment by clustering the segment colors according to chromaticity and local pixel statistics, and selecting color representatives. We used the k-means clustering method [19][20], with $K=20$, which proved to be sufficient for representing the colors of a segment. The clustering process is performed not only on the chromaticity values but also on the textural properties of the pixels for two reasons. Firstly, the same color may appear in different places in the texture, usually with a different value of luminance. Thus, color information is not enough to represent the segment. Secondly, the IR segments have no chromaticity, and the only mutual information for correct allocation from the color image is derived by using the brightness local statistics (i.e., texture) for both images. The local textural properties we used for clustering are pixel local mean, range, and standard deviation, computed in the pixel neighborhood, and also a local binary pattern (LBP) descriptor [21]. The LBP maps the local gradients of each pixel into a single equivalent value, and hence strongly represents the local textural property by a single value. We chose the LBP descriptor over the HOG one or other texture features at this stage of the algorithm because of its low computation cost. The basic LBP value for each pixel is computed as follows:

$$LBP(C) = \sum_{i=0}^{N-1} 2^i \cdot R_i, \quad (2)$$

Where C is the value of the pixel of interest, R_i is a binary value (has the value of 1 if $R_i > C$ and 0 otherwise), and N is the number of pixels in neighborhood of the pixel C . Here, we use $N = 8$, and the pixels are ordered clockwise, where $i=0$ corresponds to the top left most pixel. The outcome of the codebook creation is a representative matrix that contains sufficient color values in its rows to span the chromatic values (α, β) of the segment, while the rest of the columns are the local features parameters of each representative in the codebook. The structure of the codebook is as follows:

$\{\alpha \text{ values}, \beta \text{ values}, \text{mean}, \text{range}, \text{standard deviation}, \text{LBP}\}$

F. Pixels Matching and Chroma Transformation

To complete the colorization process, for each IR segment we use the codebook of the corresponding color segment in order to match the IR image pixels with their most similar codebook textural values. We then transfer the matched chromatic values, α and β , to the IR pixel. The original luminance values of the IR image are kept, and the result is a colored IR image in $\alpha\beta$ color space. Finally, the IR colored image is transformed back to the RGB color space.

III. SIMULATION RESULTS

For our experiments we used images of natural scenes, with a resolution of 640×480 pixels. The database contains six groups of common natural scene images that were collected

from the Internet: (1) forest, (2) grass and trees, (3) hills, (4) savannah, (5) tundra and (6) woods. Each group contains 10 images, for a sum total of 60 images.

Some of the IR images (rows 1-3 of Fig. 2) that were used were acquired by an uncooled thermal IR single-band Eyer25-Opgal camera. The scenes were taken from distances of about 10 to 40 meters during Israeli midsummer's day. The rest of the images are from the OTCBVS database [22].

Quality assessment of fake colorization is subjective and hard to quantify. In an attempt to perform a relevant comparison with previous works, we define the following criteria of quality: (1) similar objects retain similar colors, (2) objects do not obtain unnatural colors, i.e., red sky, blue trees, etc.

Figure 2 presents several examples of colorization results. Columns (a) and (b) depict the IR target image and the selected color source image respectively, column (c) is the result obtained by using Toet's single-band algorithm for colorization [5], and column (d) corresponds to results obtained by using the proposed colorization technique. It can be seen that the selected source images have a high degree of resemblance to the IR images in their type of scenery and textural content. Additionally, in terms of the quality criteria we defined, we have found that our colorization process yields more natural colorization results, and that objects of similar texture retain similar colors. A good example for the algorithm's robustness to outliers can be seen in the last row image, in which Toet's technique allowed the road to be painted blue, while our algorithm gave the road its natural gray color.

IV. CONCLUSION

In this paper, we have proposed a novel method for colorizing single-band IR images, based on the colors of an image with similar textures. There are three main novelties in the proposed technique. (1) The selection of the color source image is performed automatically from a database of color images. (2) Colorization is performed according to a local chromatic codebook, established by texture-based segmentation. (3) Local textural features are used for pixel matching. We found that the use of texture-based segmentation narrows down the possible matching selection, and therefore local characteristics can be better expressed. In order to check our method's effectiveness we compared our results with [5] algorithms' outcomes and our results show a more natural appearance.

V. ACKNOWLEDGMENT

We would like to thank the staff of the Signal & Image Processing Lab (SIPL) for their support and comments on this paper - Prof. David Malah, Yair Moshe and Nimrod Peleg. We would also like to acknowledge Senso-Optics Ltd for their help and advice during the research. Last but not least we would like to thank Guy Likver, Arthur and Elie Dordek for their help, advice and constructive comments.

REFERENCES

- [1] D. Mapelli and M. Behrmann, "The role of color in object recognition: Evidence from visual agnosia," *Neurocase*, vol. 3, no. 4, pp. 237-247, 1997.
- [2] J. E. Joseph and D. R. Proffitt, "Semantic versus perceptual influences of color in object recognition.," *Journal of experimental psychology. Learning, memory, and cognition*, vol. 22, no. 2, pp. 407-29, Mar. 1996.
- [3] E. A. Essock, M. J. Sinai, J. S. McCarley, W. K. Krebs, and J. Kevin DeFord, "Perceptual Ability with Real-World Nighttime Scenes: Image-Intensified, Infrared, and Fused-Color Imagery," *Human Factors: The Journal of the Human Factors and Ergonomics Society*, vol. 41, no. 3, pp. 438-452, Sep. 1999.
- [4] D. Scribner, P. Warren, and J. Schuler, "Extending color vision methods to bands beyond the visible," *Proceedings IEEE Workshop on Computer Vision Beyond the Visible Spectrum: Methods and Applications (CVBS'99)*, pp. 33-40.
- [5] A. Toet, "Colorizing single band intensified nightvision images," *ELSEVIER*, vol. 26, no. 1, pp. 15-21, Jan. 2005.
- [6] S. Sun, Z. Jing, and G. Liu, "Transfer color to night vision images," *Chinese Optics Letters*, 2005.
- [7] M. a. Hogervorst and A. Toet, "Fast natural color mapping for night-time imagery," *Information Fusion*, vol. 11, no. 2, pp. 69-77, Apr. 2010.
- [8] Y. Zheng and E. Essock, "A local-coloring method for night-vision colorization utilizing image analysis and fusion," *Information Fusion*, vol. 9, no. 2, pp. 186-199, Apr. 2008.
- [9] A. Levin, D. Lischinski, and Y. Weiss, "Colorization using optimization," in *ACM Transactions on Graphics (TOG)*, 2004, vol. 23, no. 3, pp. 689-694.
- [10] M. F. Abdulhalim and Z. A. Mejbil, "Automatic Colorization without Human Intervention," *Science*, vol. 1, no. 1, pp. 62-65, 2008.
- [11] W. Pyramid, Y. Xu, X. Yang, H. Ling, and H. Ji, "A New Texture Descriptor Using Multifractal Analysis in Multi-orientation," *Science*, no. 60603022, pp. 161-168, 2010.
- [12] Y. Xu, H. Ji, and C. Fermüller, "Viewpoint Invariant Texture Description Using Fractal Analysis," *International Journal of Computer Vision*, vol. 83, no. 1, pp. 85-100, Feb. 2009.
- [13] Y. Xu, S. Huang, and H. Ji, "Combining powerful local and global statistics for texture description," *Computer Vision and*, pp. 573-580, 2009.
- [14] C. Fermuller, "A Projective Invariant for Textures," *2006 IEEE Computer Society Conference on Computer Vision and Pattern Recognition - Volume 2 (CVPR'06)*, vol. 2, pp. 1932-1939, 2006.
- [15] B. B. Mandelbrot, *The Fractal Geometry of Nature*, vol. 51, no. 3. Freeman, 1983, p. 468.
- [16] D. L. Ruderman, T. W. Cronin, and C.-chin Chiao, "Statistics of cone responses to natural images: implications for visual coding," *America*, vol. 15, no. 8, pp. 2036-2045, 1998.
- [17] E. Reinhard and M. Adhikhmin, "Color transfer between images," *and Applications, IEEE*, no. October, pp. 34-41, 2001.
- [18] N. Dalal, "Histograms of oriented gradients for human detection," *2005. CVPR 2005. IEEE Computer Society*, vol. 1, pp. 886-893, 2005.
- [19] G. A. F. Seber, *Multivariate Observations*, vol. 14, no. Book, Whole. Wiley, 1984, p. 720.
- [20] H. Spath, "Cluster Dissection and Analysis: Theory, FORTRAN Programs and Examples," *Halsted Press*, 1985.
- [21] T. Maenpaa, "The Local Binary Pattern Approach to Texture Analysis -- Extensions and Applications," University of Oulu, 2003.
- [22] "OTCBVS Benchmark Dataset Collection." [Online]. Available: <http://www.cse.ohio-state.edu/otcbvs-bench/>.

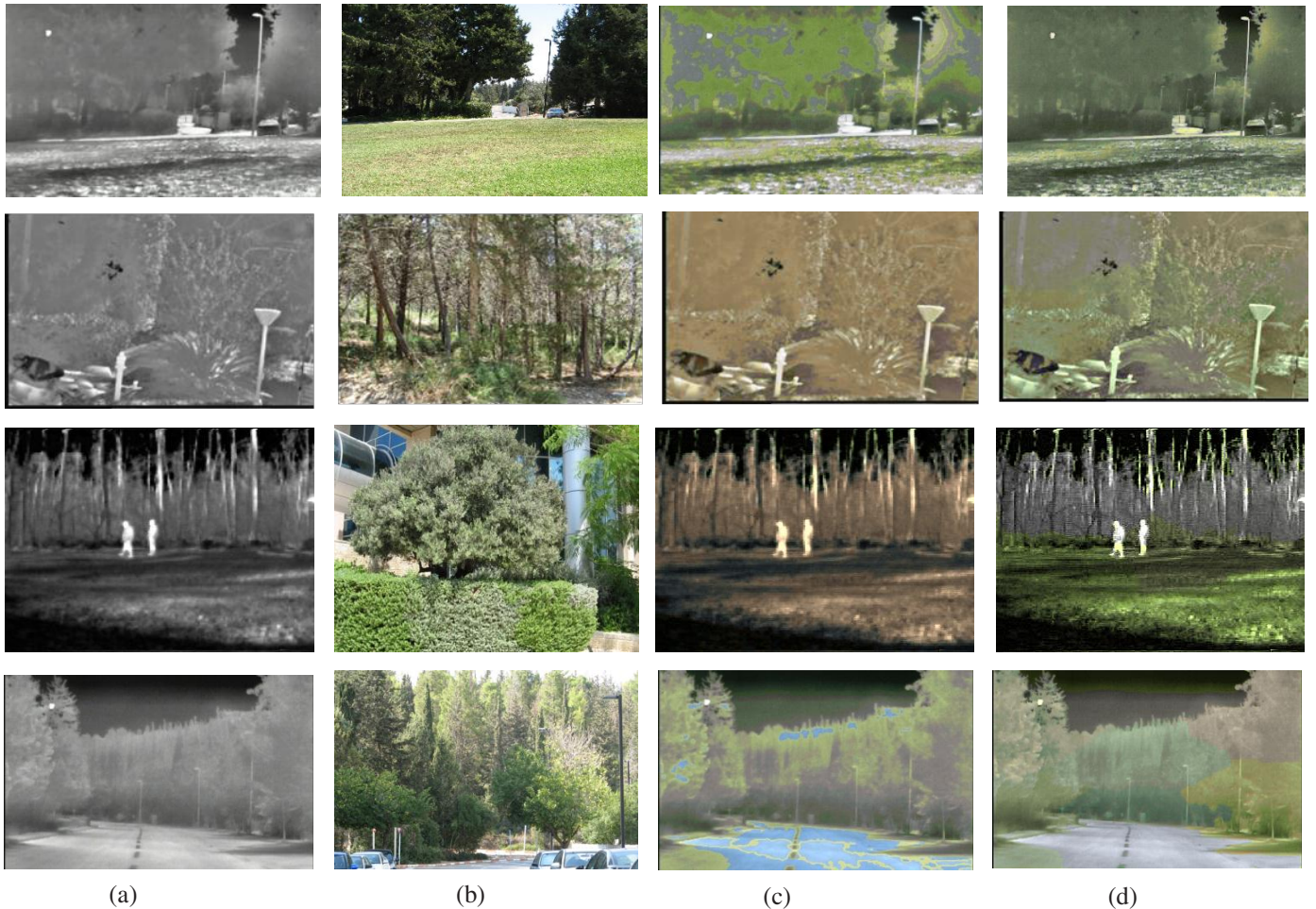


Figure 2- (a) target IR images, (b) color source image, (c) colorization obtained of [5], (d) colorization obtained with proposed technique. The results show that our proposed technique indeed achieve more natural coloring.